Development 134, 1583-1592 (2007) doi:10.1242/dev.000703

Activities of N-Myc in the developing limb link control of skeletal size with digit separation

Sara Ota[1,*], Zi-Qiang Zhou[1,*], Doug R. Keene[1], Paul Knoepfler[2] and Peter J. Hurlin[1,3,†]

The developing limb serves as a paradigm for studying pattern formation and morphogenetic cell death. Here, we show that conditional deletion of N-Myc (Mycn) in the developing mouse limb leads to uniformly small skeletal elements and profound soft-tissue syndactyly. The small skeletal elements are associated with decreased proliferation of limb bud mesenchyme and small cartilaginous condensations, and syndactyly is associated with a complete absence of interdigital cell death. Although Myc family proteins have pro-apoptotic activity, N-Myc is not expressed in interdigital cells undergoing programmed cell death. We provide evidence indicating that the lack of interdigital cell death and associated syndactyly is related to an absence of interdigital cells marked by expression of Fgfr2 and Msx2. Thus, instead of directly regulating interdigital cell death, we propose that N-Myc is required for the proper generation of undifferentiated mesenchymal cells that become localized to interdigital regions and trigger digit separation when eliminated by programmed cell death. Our results provide new insight into mechanisms that control limb development and suggest that defects in the formation of N-Myc-dependent interdigital tissue may be a root cause of common syndromic forms of syndactyly.

KEY WORDS: Myc, N-Myc, Limb, Syndactyly, Apoptosis, Interdigital, Mouse

INTRODUCTION

Vertebrate limbs emerge along the embryonic body as buds of rapidly dividing mesenchymal cells covered by a layer of ectoderm. Within limb bud mesenchyme are cells that differentiate into connective tissues, including tendons and ligaments, and chondrocytes that give rise to the cartilage templates that prefigure the limb skeleton. Chondrocytes develop from mesenchymal condensations in the early limb bud and are subsequently patterned into the different cartilage segments (reviewed by Mariani and Martin, 2003; Niswander, 2003; Tickle, 2003). Generating and fixing the positional identity of limb bud cells to produce the complex pattern of the developing cartilage templates requires the coordination of at least three organizing centers. The first organizing center that forms is the apical ectodermal ridge (AER), a morphologically distinct epithelium located at the distal margin of the limb bud that produces fibroblast growth factors (FGFs) required for sustained proximodistal (PD, shoulder to digits) growth. The zone of polarizing activity (ZPA) forms soon after and directs anteroposterior (AP, little finger to thumb) through the secretion of Sonic hedgehog (Shh) from posterior mesenchyme. Finally, the dorsoventral axis of the limb is patterned through Wnt signaling emanating from dorsal ectoderm. In addition to controlling axis formation, elements of these pathways appear to be integrated into the program that regulates cell death of interdigital mesenchyme (IDM), which functions in the process of digit separation in vertebrate species with free digits.

[1]Shriners Hospitals for Children Portland, 3101 SW Sam Jackson Park Road, Portland, OR 97239, USA. [2]Department of Cell Biology and Human Anatomy, Davis School of Medicine, 3301 Tupper Hall, University of California, Davis, CA 95616, USA. [3]Department of Cell and Developmental Biology, Oregon Health and Science University, 3181 SW Sam Jackson Park Road, Portland, OR 97239, USA.

*These authors contributed equally to this work
†Author for correspondence (e-mail: pjh@shcc.org)

Accepted 8 February 2007

The Myc family proteins N-Myc (also known as Mycn – Mouse Genome Informatics) and c-Myc (also known as Myc – Mouse Genome Informatics) play essential roles during vertebrate development, as embryos lacking N-Myc or c-Myc die by embryonic day (E) 11.5 and E10.5, respectively (reviewed by Hurlin, 2005; Murphy et al., 2005). Lethality is associated with defective formation of many organs and is linked to a general failure of different cell populations to sustain proliferation. The characterization of mice following conditional, tissue-specific deletion of N-Myc and c-Myc has further demonstrated their essential roles in maintaining progenitor populations and controlling the balance between cell proliferation and differentiation. For example, N-Myc is required in neuronal and lung progenitor populations to promote their proliferation, prevent their differentiation and maintain their plasticity (Knoepfler et al., 2002; Okubo et al., 2005).

The important activities of c-Myc and N-Myc in regulating cell proliferation and differentiation during embryonic development are consistent with their well-characterized roles in tumor formation. Forced expression of Myc family proteins generally prevents cell differentiation, ultimately leading to uncontrolled proliferation and tumorigenesis in a wide variety of settings. However, in many cell types, such uncontrolled proliferation is counteracted by a high rate of apoptosis (Nilsson and Cleveland, 2003). While it is well documented that forced expression of Myc family proteins can trigger apoptosis, there is little or no direct evidence indicating that they play normal physiological roles in programmed cell death. The possibility that N-Myc might regulate programmed cell death of IDM was suggested by the finding that haploinsufficiency of N-Myc causes Feingold syndrome (van Bokhoven et al., 2005), a pleomorphic disease syndrome often characterized by a mild form of syndactyly (Celli et al., 2003). Syndactyly is a relatively common human birth defect, and it is widely thought that defects in molecular pathways controlling programmed cell death of interdigital tissue are responsible. Thus, it is of considerable interest to determine the possible role that N-Myc plays in interdigital cell death.

In addition to a potential role of N-Myc in regulating interdigital cell death, early studies of N-Myc null mice suggest that N-Myc is important in early limb development. Limb buds of N-Myc null embryos were small, and failed to develop distal skeletal elements when cultured in vitro, leading to the conclusion that N-Myc is required for proliferation of limb mesenchyme and sustained PD limb growth (Sawai et al., 1993). However, germline deletion of N-Myc causes lethality at an early stage of limb development, raising the possibility that deficiencies in other crucial supporting systems within the embryo regulated by N-Myc are responsible for the small limb buds. Further, the limb bud culture experiments, necessitated by the early lethality, probably do not accurately recapitulate normal development. The lethality of N-Myc null mice also precluded any investigation of the role N-Myc might play in later events of limb morphogenesis, including interdigital programmed cell death.

To better define the role of N-Myc in limb development, we re-examined limb buds of N-Myc null mice and analyzed limb development following conditional deletion of N-Myc in the early limb bud. We found that N-Myc deficiency caused diminished cell proliferation, particularly in the early limb bud, and caused a relatively uniform reduction in the size of all skeletal elements. Most striking however, was a complete absence of programmed cell death of interdigital tissue and the development of profound soft-tissue syndactyly. Surprisingly, N-Myc expression is excluded from cells undergoing cell death and instead of regulating programs that control apoptosis, our results suggest that syndactyly is caused by a failure to produce N-Myc-dependent interdigital cells, of which the elimination by cell death mediates digit separation.

MATERIALS AND METHODS

Mice

Intercrosses between *N-Myc*$^{f/f}$ (Knoepfler et al., 2002) and Prx1-Cre mice (Logan et al., 2002) on a mixed background of C57BL/6 and 129 yielded PC-*NMyc*$^{f/f}$ mice. Mice and embryos were genotyped as previously described (Knoepfler et al., 2002; Logan et al., 2002).

In situ hybridization

In situ hybridization of whole embryos and sections was performed using digoxigenin-UTP-labeled riboprobes as previously described (Brent et al., 2003).

BrdU incorporation

BrdU (Sigma) labeling (1.5 hours) was performed as described by Queva et al. (Queva et al., 1998) using BD Biosciences BrdU In Situ Detection Kit. Anti-BrdU stained sections were counterstained with Hematoxylin.

Immunohistochemistry and electron microscopy

Embryos were fixed overnight in 4% paraformaldehyde and imbedded in OCT. Frozen sections were blocked with 20% donkey or goat serum in PBS followed by overnight incubation of primary antibodies [anti-E-cadherin (Santa Cruz), anti-cyto pan keratin (Sigma), Pecam (Santa Cruz)] at 4°C. Cy3-conjugated donkey anti-mouse F(ab)$_2$ (Jackson ImmunoResearch Laboratories) and goat anti-rabbit IgG (Alexa Fluor 488, Molecular Probes) were used as secondary antibodies. For TEM, E13.5 forelimbs were fixed in 1.5% glutaraldehyde/1.5% paraformaldehyde containing 0.05% tannic acid and processed as previously described (Sakai et al., 1986).

Skeletal preparation

De-skinned embryos and newborns were stained with 0.05% Alcian Blue and 0.015% Alizarin Red in 70% ethanol and 13% glacial acetic acid for 3 days, cleared in 0.5% KOH overnight and stored in glycerin.

Cell death assays

Transverse sections of embryos were assayed by TUNEL using the Roche In Situ Cell Death Detection Kit. Detection of cell death by LysoTracker (Molecular Probes) staining was carried out according to the protocol of Zucker et al. (Zucker et al., 1999).

RESULTS

Disruption of N-Myc does not prevent formation of the AER and ZPA

To delete *N-Myc* in limb bud mesenchyme, mice containing conditional, LoxP/Cre *N-Myc* alleles (Knoepfler et al., 2002) were mated with Prx1-Cre transgenic mice (Logan et al., 2002). Logan et al. (Logan et al., 2002) showed that Prx1-Cre is active in the emerging forelimb bud mesenchyme at E9.5 and hindlimb mesenchyme at E10.5. The region targeted by Prx1-Cre appears to completely overlap with the regions of N-Myc expression in the early limb bud (Sawai et al., 1990; Kato et al., 1991; Queva et al., 1998) (see Fig. 2A). Using Cre-reporter mice (Soriano, 1999), we found Prx1-Cre to also be active in lateral mesenchyme at E8.5-9, which coincides with the emergence of the forelimb bud (not shown). When compared with N-Myc germline null and control Prx1-Cre (PC) embryos, the forelimb and hindlimb buds of Prx1-Cre-*N-Myc*$^{f/f}$ (PC-*NMyc*$^{f/f)}$ embryos at E10.5 were intermediate in size (Fig. 1A and not shown). However, whereas the body size of PC-*NMyc*$^{f/f}$ embryos was otherwise close to that of control embryos, the small limb buds of *N-Myc*$^{-/-}$ embryos corresponded to their overall small embryonic size (Fig. 1A). Furthermore, while *N-Myc* null embryos died by E11.5, PC-*NMyc*$^{f/f}$ embryos were viable and gave rise to fertile adults. Thus, the effect of N-Myc deletion by Prx1-Cre on limb development can be attributed to the intrinsic function of N-Myc in this process and not to N-Myc-dependent regulation of extrinsic factors that might influence limb development.

The small limb buds of *N-Myc* null embryos and PC-*NMyc*$^{f/f}$ embryos might be due to predicted effects of N-Myc deficiency on cell proliferation (see more below), or defects in establishing the early organizing centers that regulate cell proliferation. However, expression of *Fgf8*, marking the formation of the AER, and *Sonic Hedgehog* (*Shh*), marking formation of the ZPA, were clearly present and appeared correctly positioned in limb buds of *N-Myc* null and PC-N*Myc*$^{f/f}$ embryos (Fig. 1B). *Gremlin*, which is a target of Shh signaling involved in feedback regulation between the ZPA and AER (Zuniga et al., 1999; Capdevila et al., 1999), is also present in both *N-Myc* null and PC-*NMyc*$^{f/f}$ limb buds, but its expression is expanded (Fig. 1B). Consistent with this finding, expression of *Fgf4* is elevated in the AER of N-Myc-deficient limb buds (Fig. 1B). However, *Gremlin* and *Fgf4* expression is extinguished at later stages, as in control limb buds (Fig. 6B and not shown). Bone morphogenetic protein 4 (*Bmp4*), which is expressed in both the AER and the ZPA, and *Hand2*, which marks cells competent to become the ZPA (te Welscher et al., 2002), were expressed in PC-*NMyc*$^{f/f}$ and *N-Myc* null limb buds at their proper locations (Fig. 1B). However, *Hand2* appeared to be downregulated in N-Myc-deficient limb buds. Finally, *Gli3*, which is restricted to anterior mesenchyme at E10.5, at least in part by *Hand2* (te Welscher et al., 2002), had an anterior expression domain in N-Myc-deficient limb buds, but was strongly downregulated (Fig. 1B). Although *Hand2* and *Gli3* were expressed at low levels in N-Myc-deficient limb buds at E10.5, their levels and position were comparable to control embryos at E11.5 (not shown). Taken together, these results indicate that the AER and ZPA are formed in N-Myc-deficient limb buds, but that at least some of their activities are transiently disrupted or delayed.

N-Myc regulates cell proliferation in limb bud mesenchyme

The close association of Myc proteins with cell proliferation prompted an examination of the relationship between cell proliferation and *N-Myc* expression in the limb bud. Consistent with

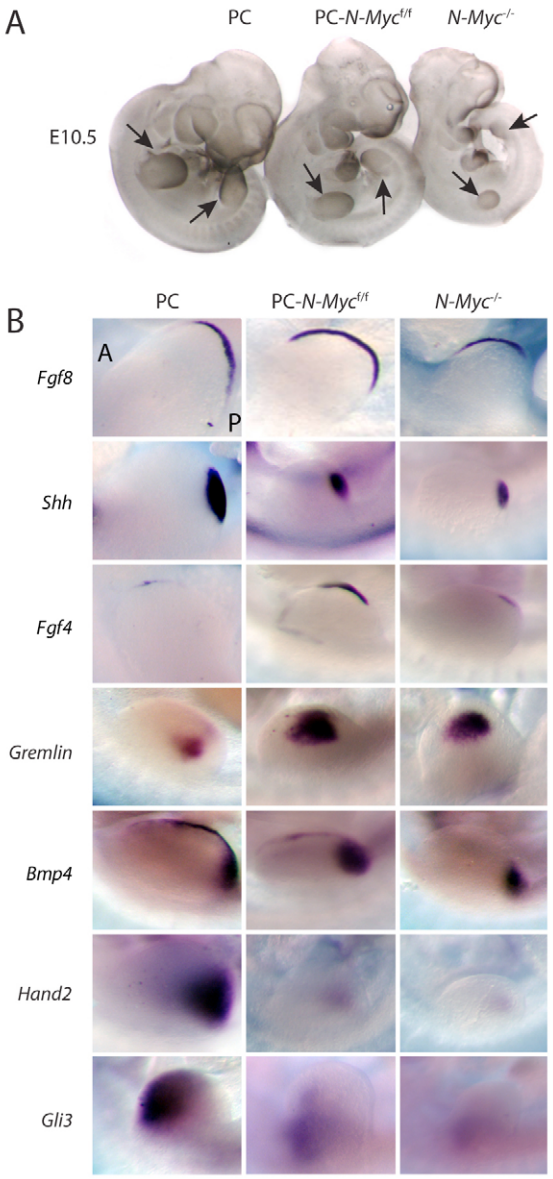

Fig. 1. Effect of N-Myc deficiency on mouse limb bud formation. (**A**) Comparison of PC control embryos with PC-*NMyc*$^{f/f}$ and *N-Myc* null embryos at E10.5. Arrows indicate forelimb and hindlimb buds. Note that *N-Myc* null embryos die between E10.5 and 11.5. (**B**) Representative whole-mount in situ hybridization results showing forelimb expression of the indicated genes at E10.5. At least three sets of embryos were used for each probe. A, anterior; P, posterior.

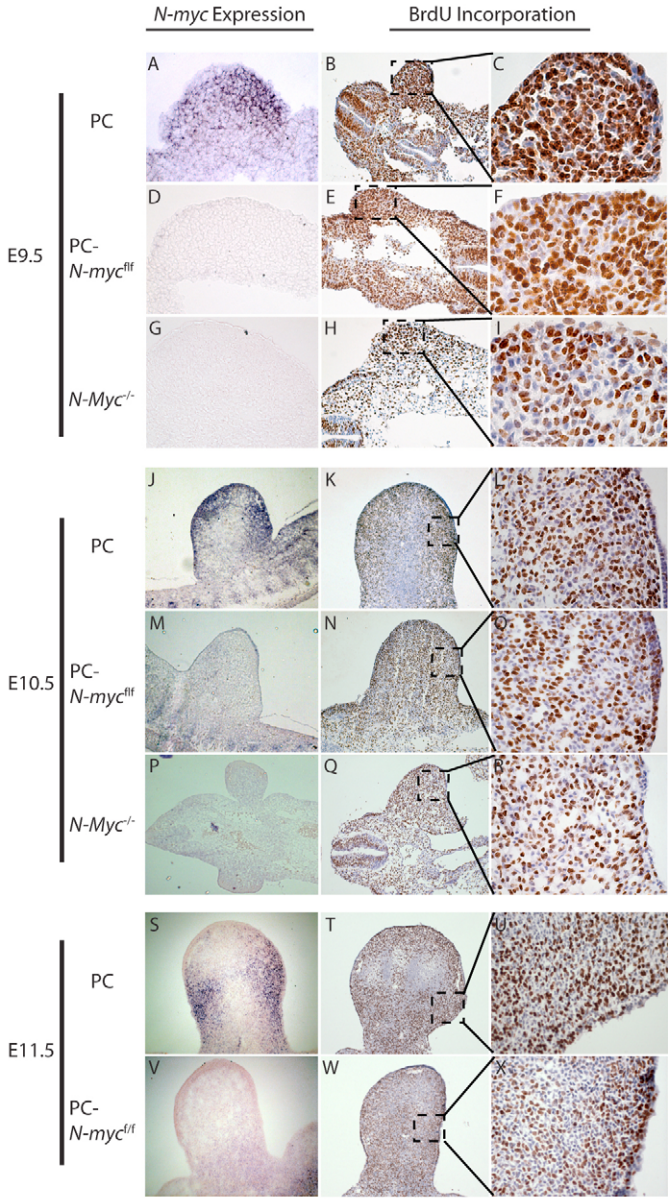

Fig. 2. Decreased proliferation in mouse limb bud mesenchyme caused by loss of N-Myc. (**A-X**) *N-Myc* expression is shown by in situ hybridization of transverse sectioned limb buds from PC, PC-*NMyc*$^{f/f}$ at E9.5, 10.5 and 11.5 as indicated. *N-Myc*$^{-/-}$ embryos were analyzed only at E9.5 and 10.5 due to lethality by E11.5. Transverse limb bud sections were stained for BrdU incorporation (brown) and counterstained with Hematoxylin (blue). The boxed regions, representing areas in which N-Myc is expressed or predicted to be expressed in the mutants, are shown at higher magnification (40× of E9.5 sections and 20× of E10.5 and 11.5 sections) in panels on the right.

previous results (Kato et al., 1991), *N-Myc* was expressed in limb bud mesenchyme at E9.5, with highest levels in the posterior bud and not expressed in limb bud ectoderm (Fig. 2A). In contrast, *N-Myc* expression was absent in most, if not all, mesenchymal cells of PC-*NMyc*$^{f/f}$ limb buds (Fig. 2D) and was absent as expected in germline null limb buds at E9.5 (Fig. 2G). The loss of *N-Myc* expression in PC-*NMyc*$^{f/f}$ limb buds is consistent with robust Prx1-Cre activity at the earliest stages of limb bud outgrowth (Logan et al., 2002) (and data not shown). The absence of *N-Myc* in PC-*NMyc*$^{f/f}$ and *N-Myc* null limb buds at E9.5 was associated with a decline in cell proliferation, as measured by the percentage of cells that incorporated BrdU compared to control limb buds (Fig. 2B,C,E,F,H,I and Table 1). The decrease in BrdU incorporation caused by loss of N-Myc corresponded to a decrease in cell density (Table 1).

At E10.5, control limb buds showed continued expression of *N-Myc* in distal mesenchyme underlying the AER, but it was strongly regionalized to distal anterior and posterior regions (Fig. 2J). *N-Myc* expression overlapped with regions in which cells were undergoing DNA replication at E10.5 (Fig. 2K,L) and was excluded from central limb bud regions in which precartilaginous mesenchymal

Table 1. Summary of BrdU incorporation and cell density in limb buds of control, PC-*NMyc*$^{f/f}$ and *N-Myc* null mice

	% BrdU positive			Cells/equal area		
Stage/position	Wild type	PC-*NMyc*$^{f/f}$	N-Myc$^{-/-}$	Wild type	PC-*NMyc*$^{f/f}$	N-Myc$^{-/-}$
E9.5	80±2.5	72±2.2**	70±1.8**	321±12	293±13**	165±8*
E10.5/Distal	62±1.9	60±1.8***	60±1.5***	341±9	290±10**	170±7*
E10.5/Posterior	63±1.3	59±2.1***	NA	344±12	265±13*	NA
E10.5/Anterior	65±1.6	59±1.8***	NA	351±13	308±9**	NA
E11.5/Distal	63±1.4	58±1.2***	NA	394±23	320±18**	NA
E11.5/Posterior	66±2.1	61±1.8***	NA	401±26	340±12**	NA
E11.5/Anterior	65±1.6	62±1.9***	NA	374±20	327±18**	NA

Cell counts performed on limb buds of E9.5 embryos and N-Myc null embryos encompassed the entire limb bud. Otherwise, cell counts were performed on comparable distal, posterior and anterior regions as indicated. Cell counts were determined from stained nuclei within tissue sections derived from three embryos and standard deviations are shown. *P* values, *<0.001, **<0.01, ***>0.01. NA, not applicable.

condensations (marked by blue Hematoxylin staining) were forming and BrdU incorporation was low (Fig. 2K,L). *N-Myc* transcripts were undetectable in PC-*NMyc*$^{f/f}$ limb buds at E10.5 (Fig. 2M), as well as N-Myc null limb buds (Fig. 2P), both of which exhibited a more uniform distribution of BrdU-positive cells (Fig. 2N,O,Q,R). The more uniform distribution appears to correspond to a strong reduction in the size of the centrally located precartilaginous condensation, where BrdU incorporation is normally low (compare Fig. 2N,Q with 2K). However, the percentage of BrdU-positive cells and the cell density in specific distal, posterior and anterior regions was consistently lower in PC-*NMyc*$^{f/f}$ and *N-Myc* null limb buds compared with control limb buds (Fig. 2L,O,R and Table 1). At E11.5, *N-Myc* expression showed a strong anterior and posterior bias and overlapped with regions undergoing cell proliferation (Fig. 2S-U). Similar to the situation at E10.5, Prx1-Cre deletion of N-Myc caused a decrease in the percentage of cells that incorporated BrdU and a decrease in cell density in regions where N-Myc expression was lost (Fig. 2V-X).

Levels of cell death, as measured by TUNEL, in the mutant limb buds was very low or non-detectable between E9.5 and 11.5 and no different from control limb buds (not shown). Taken together, these results suggest that the reduced size and cell density of PC-*NMyc*$^{f/f}$ and *N-Myc* limb buds is attributable to a decrease in proliferation of undifferentiated limb bud mesenchyme, particularly in the very early limb bud around E9.5. Further, the altered distribution of BrdU-positive cells was associated with a decrease in the size of the central mesenchymal condensation between E10.5 and 11.5, suggesting that N-Myc is an important regulator of the number or behavior of progenitor cells that give rise to the precartilaginous condensations.

Importantly, neither *c-Myc* nor *L-Myc* (*Mycl1* – Mouse Genome Informatics) expression appeared to overlap with *N-Myc* expression in the developing limb, and no compensatory upregulation or changes in their expression pattern was seen in N-Myc-deficient limb buds (data not shown).

Loss of N-Myc leads to decreased skeleton size and defective digit formation

Staining with cartilage-specific Alcian Blue and bone-specific Alizarin Red at E15.5 revealed that early limb skeletal elements of N-Myc-deficient limbs were 20-40% smaller (length and diameter) than those of control littermates (Fig. 3A-C and data not shown). An exception is the most posterior digit (digit 5), the length (but not diameter) of which was relatively unaffected. Notably, the reduced size of limb elements was largely proportional to each other. Further, the most proximal upper limb element, the scapula, which forms in lateral mesenchyme and not the limb bud proper, was reduced in size (Fig. 3A), consistent with Prx1-Cre activity in presumptive limb regions of lateral mesenchyme. The small limb skeletal elements were maintained during embryonic development (Fig. 3B,C) and into young mice, although the size differential with control mice was slightly decreased in juveniles (not shown).

Little is known about the nature of mesenchymal cells that give rise to chondrocytes, but their development and pool size appeared to be linked to formation of the AER and production of AER-derived FGFs, particularly Fgf8 (Niswander, 2003; Tickle, 2003). Although N-Myc deficiency did not disrupt expression of *Fgf8* and formation of the AER or ZPA (Fig. 1B), it had a marked effect on expression of *Sox9*. Sox9 is a marker of precartilaginous condensations and is required for development of chondrocytes (Bi et al., 1999). *Sox9* was very low in N-Myc-deficient limb buds at E10.5 and continued to be low through E13.5 (Fig. 3D). The low *Sox9* levels corresponded to a reduction in the size of condensations observed at E10.5 and 11.5 (Fig. 2G,S). As illustrated in sections through the developing digits at E13.5 (Fig. 3D), the low *Sox9* expression corresponded to small cartilaginous elements. Similarly, expression of other chondrocyte markers, including *Noggin* (Fig. 3E) and Collagen II (not shown), was diminished in N-Myc-deficient limbs and probably reflects a smaller domain of chondrogenic mesenchyme in the developing skeleton. Because *N-Myc* expression appeared not to overlap with *Sox9*-positive condensing mesenchyme in the early limb bud (compare Fig. 2A,M with Fig. 3D), these data, taken together with the results of BrdU-incorporation assays, further suggest that N-Myc regulates the size and/or behavior of undifferentiated limb bud mesenchyme that gives rise to the Sox9-positive limb bud condensation. Thus, the small skeletal elements cause by loss of N-Myc may reflect a significant reduction in the initial pool of chondrogenic progenitor cells.

In addition to causing small skeletal elements, N-Myc deficiency disrupts digit joint formation (Fig. 3B,C). Digits 2 to 5 had only one distinct joint distal to the metacarpal joint, when they should have two, and all of other digit joints that did form, including the metacarpal joints, were poorly formed. Expression of *Gdf5*, a BMP family member that marks presumptive joints and is required for proper joint formation (Archer et al., 2003) was weak in PC-*NMyc*$^{f/f}$ limbs and lacked the prominent distal digit expression seen in control embryos at E12.5 (Fig. 3F). *Gdf5* was also very low at presumptive phalangeal joints at E13.5 and 14.5 (Fig. 3F). Gdf5 has strong effects on chondrocyte proliferation (Archer et al., 2003) and its weak expression may contribute to reduced digit (and other skeletal element) size and associated joint defects. Alternatively, its weak expression may simply be a consequence of reduced numbers of chondrocytes or other cell types in digit primordia that normally express Gdf5.

N-Myc-deficient forelimbs also exhibited fusions of digit 5 and digit 4 at their metacarpal bases (53/53) and between the metacarpal bases of digits 1 and 2 (26/53) (Fig. 3B,C and not shown). Fusion

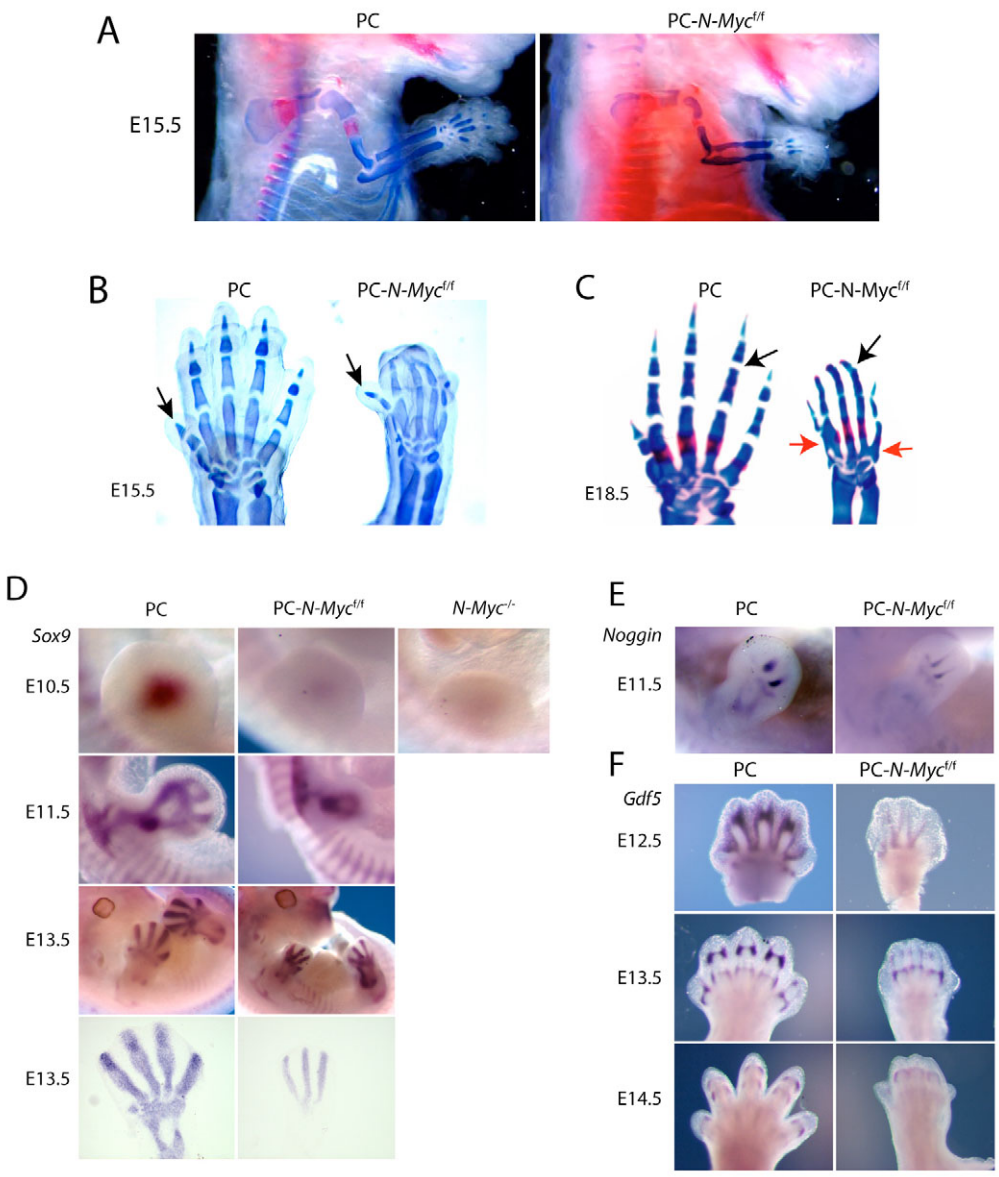

Fig. 3. Effects of N-Myc deficiency on the size and pattern of the limb skeleton. (**A**) Alcian Blue (staining for cartilage) and Alizarin Red (staining for bone) staining of PC and PC-*NMyc*$^{f/f}$ mouse embryos at E15.5. (**B**) E15.5 autopods stained with Alcian Blue. Note that the phalangeal elements of digit 1 (thumb, black arrows) are longer in PC-*NMyc*$^{f/f}$ embryos and resemble those of the most posterior digit (digit 5 or little finger). (**C**) The distal skeleton of E18.5 PC and PC-*NMyc*$^{f/f}$ embryos stained with Alcian Blue and Alizarin Red. Note the lack of well-defined joints (black arrows), or absence of joints, in the digits of PC-*NMyc*$^{f/f}$ embryos. Note also the bony fusions that occur at the base of the anterior and posterior digits of the PC-*NMyc*$^{f/f}$ autopod (red arrows). (**D**) Analysis of *Sox9* expression, a marker of cartilage growth and development, by whole-mount and section in situ hybridization at the indicated embryonic stages. (**E**) Whole-mount in situ hybridization showing *Noggin* expression at E11.5. (**F**) Expression of *Gdf5*, a marker of joint development, at the indicated embryonic stages.

between the distal tips of the central three digits was also frequent (46/53), but whereas metacarpal fusions were apparent by E14.5, the distal fusions occurred at later stages (not shown).

Absence of interdigital and joint cell death in N-Myc-deficient limbs

Perhaps the most striking feature of PC-*NMyc*$^{f/f}$ limbs is a profound soft tissue syndactyly, particularly in the forelimb (Fig. 4). Interestingly, whereas digits 1 (thumb) and 5 (little finger) of N-Myc-deficient forelimb buds clearly protruded from the body of the autopod at E15.5, these digits were completely enveloped in tissue by E18.5 (Fig. 4B), and remained so at 1 week of age (Fig. 4C). It is not clear why hindlimb syndactyly is less severe, but it may be due to reduced or delayed activity of *Prx1*-Cre in hindlimb relative to forelimb (Logan et al., 2002). There was no evidence of syndactyly in mice heterozygous for *N-Myc* (equivalent to Feingold syndrome in humans).

To examine the relationship between N-Myc and cell death in the autopod, *N-Myc* expression was compared to whole-mount LysoTracker and TUNEL staining (marking apoptotic cells) of limb sections at E12.5, 13.5 and 14.5, stages when interdigital cell death is most active. At E12.5 *N-Myc* expression was highest in undifferentiated mesenchyme surrounding the anterior and posterior digit condensations (i.e. primordia of digits 1 and 5) (Fig. 5A). It was expressed at relatively low levels at the tips of digit primordia and in interdigital tissue of the central digits. At E12.5, cell death was detected primarily in the AER, but also weakly in IDM (Fig. 5B,C). *N-Myc* transcripts were not detected in PC-*NMyc*$^{f/f}$ limbs at E12.5 (Fig. 5D), and apoptosis was detected only in the AER (Fig. 5E,F).

At E13.5 *N-Myc* expression was highest in peri-digital regions (Fig. 5G). In situ hybridization of distal limb sections at E13.5 confirmed peri-digital expression and absence of *N-Myc* from digit condensations (not shown). Strikingly, *N-Myc* expression was excluded from interdigital regions undergoing cell death at E13.5 (Fig. 5G-I). *N-Myc* was not detectable in PC-N*Myc*$^{f/f}$ limbs at E13.5 (Fig. 5J), and these displayed a complete absence of interdigital cell death (Fig. 5K,L).

At E14.5, digit separation was nearly complete, and *N-Myc* continued to be expressed in peri-digital regions of the separated digits but was excluded from the remaining interdigital tissue

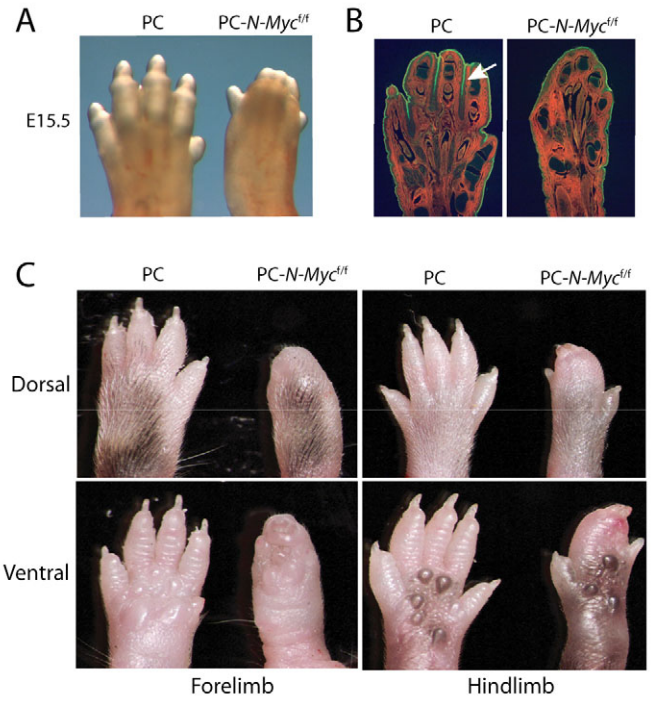

Fig. 4. N-Myc deficiency causes syndactyly. (**A**) Dorsal view of left paws (autopods) of PC and PC-*NMyc*$^{f/f}$ mouse limbs at E15.5. Note the syndactyly of the central three digits and protruding digits 1 and 5 of PC-*NMyc*$^{f/f}$ limbs. (**B**) Absence of digit individualization in N-Myc-deficient autopods at postnatal day 1. Autopods were stained for E-cadherin (green, arrow) to mark the epithelium and counterstained with a pan-cytokeratin antibody (red). (**C**) Dorsal and ventral views of forelimbs and hindlimbs of 1-week-old mice.

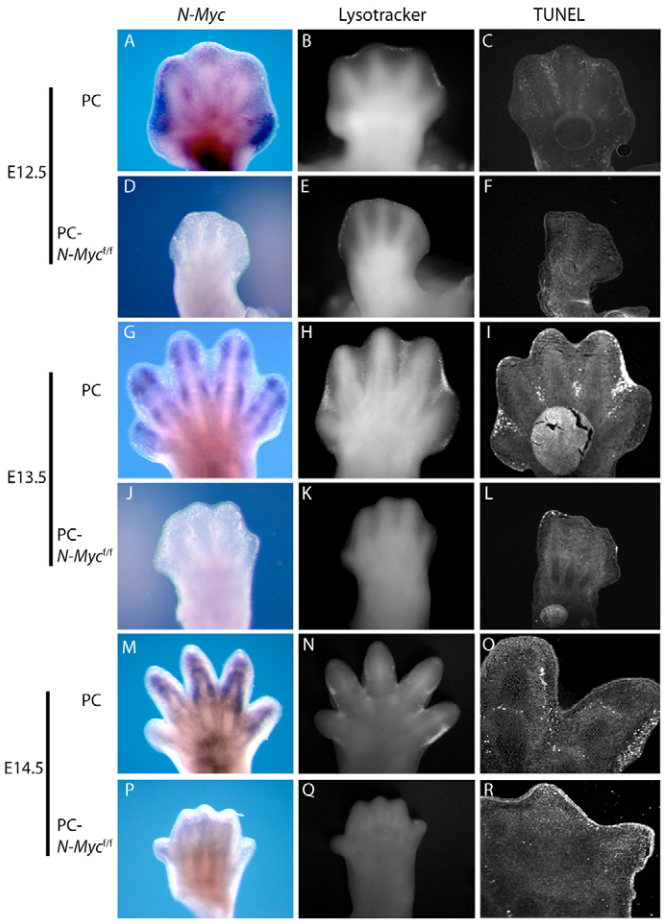

Fig. 5. The relationship between N-Myc expression and programmed cell death in the developing mouse forelimb autopod. (**A-R**) Whole-mount in situ hybridization of N-Myc is compared with whole-mount staining with LysoTracker, and sections stained for TUNEL at E12.5, 13.5 and 14.5 as indicated. For TUNEL staining at E13.5, higher magnification views of distal regions of digits 4 and 5 of *Prx1*-Cre (O) and PC-NMyc$^{f/f}$ (R) are shown.

undergoing cell death (Fig. 5M-O). It is notable that while *N-Myc* was not expressed in central interdigital regions, which undergo cell death linked to digit separation, *N-Myc* expression did appear to be coincident with some perichondrial and joint regions, where apoptosis was evident in the separated digits of E14.5 limbs (Fig. 5M-O). In PC-*NMyc*$^{f/f}$ limbs at E14.5, *N-Myc* levels were very low or undetectable (Fig. 5P), and no interdigital or joint cell death was observed (Fig. 5Q,R).

These data demonstrate that syndactyly caused by N-Myc deficiency corresponds to an absence of cell death in interdigital tissue. Importantly, the lack of correspondence between *N-Myc* expression and interdigital cell death suggests that the absence of cell death is a secondary effect of N-Myc deficiency.

Loss of N-Myc does not disrupt AER regression, but strongly affects expression of interdigital markers

Interdigital cell death occurs concomitant with regression of the AER and associated loss of AER-derived FGFs in the underlying undifferentiated mesenchyme. Forced expression of FGFs in the AER, or experimentally prolonged maintenance of the AER, prevents mesenchymal cell death and leads to syndactyly (Fallon et al., 1994; Guha et al., 2002; Wang et al., 2004; Lu et al., 2006). Therefore, one potential explanation for loss of interdigital cell death and syndactyly in N-Myc-deficient autopods is prolonged FGF signaling due to failure of AER regression. However, this appears not to be the case, as *Fgf8* expression was extinguished in ectoderm overlaying interdigital regions in both PC-NMyc$^{f/f}$ and control limbs by E13.5 (Fig. 6A). Moreover, TEM indicates that the distinctive epithelium of the AER became restricted to the distal digit tips in both PC and PC-*NMyc*$^{f/f}$ paws at E13.5 (not shown). The typically transient *Fgf4* expression in the posterior AER was not disrupted by loss of N-Myc, with expression no longer detectable by E12.5 (Fig. 6B). Thus, the absence of interdigital cell death and associated syndactyly is not due to failed AER regression or persistent ectodermal expression of Fgf8 or Fgf4.

While the specific signals that trigger interdigital cell death remain to be fully defined, BMP signaling is implicated in this process. Several BMP family members are expressed in IDM, and ectopic BMP activity in IDM can induce apoptosis (Zuzarte-Luis and Hurle, 2005). In N-Myc-deficient limbs, the interdigital and peri-digital expression of *Bmp2* and *Bmp7* was very low relative to PC limbs (Fig. 7A,B). Bmp4 expression was weakly expressed in the anterior autopod of both PC and PC-*NMyc*$^{f/f}$ limbs at E12.5 and 13.5 (not shown). *Msx2*, a key downstream target of BMP signaling was expressed strongly in the central IDM of control limbs but was very weakly expressed or absent in N-Myc-deficient limbs (Fig. 7D). The *Msx2* results suggest that either BMP signaling is strongly downregulated in the IDM, or alternatively, that IDM tissue that

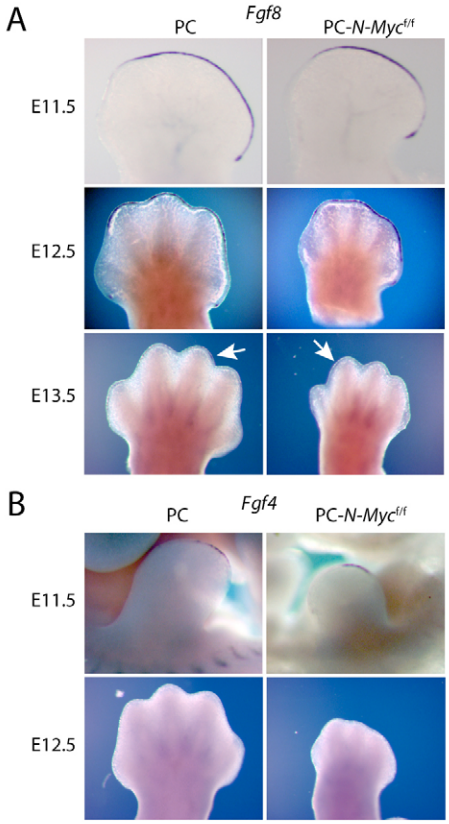

Fig. 6. N-Myc deficiency does not affect expression of *Fgf8* and *Fgf4*. Whole-mount in situ hybridization analysis of *Fgf8* (**A**) and *Fgf4* (**B**) expression in mouse forelimbs at the indicated embryonic stages. Note restriction of Fgf8 expression to epithelium at the distal tips of digits in both PC and PC-*NMyc*$^{f/f}$ embryos.

normally expresses *Msx2* is absent in PC-*NMyc*$^{f/f}$ autopods. Consistent with the latter idea, expression of *Fgfr2*, which is not known to be linked to BMP signaling in the limb, was largely lost from its well-defined central IDM domain, but not from peri-digital locations (Fig. 7E). In addition, interdigital *Twist* expression was strongly downregulated (Fig. 7F). Taken together, these results raise the possibility that the absence of interdigital cell death caused by N-Myc deficiency is due to the absence of a population of interdigital cells, marked by expression of *Fgfr2*, *Msx2* and to a lesser extent *Twist*, that are normally destined to undergo programmed cell death as a trigger for digit separation.

Absence of interdigital tissue in N-Myc-deficient paws

It was noticed that prior to digit separation, the distance between digit primordia in PC-*NMyc*$^{f/f}$ autopods was less than in control autopods. Measurements of the distance between digits at E13.5 indicated that they were at least 40% closer in PC-*NMyc*$^{f/f}$ limbs (n=6, not shown). The architecture of the autopod and interdigital tissue was further investigated at E13.5 by examining patterns of cell proliferation by BrdU incorporation. The pattern of BrdU incorporation in control PC mice revealed a distinct channel of interdigital tissue exhibiting a very low level of BrdU incorporation between adjacent perichondrial regions, where BrdU incorporation was much higher (Fig. 8A). Although it remains to be confirmed, the low-BrdU region appeared to correspond to the interdigital expression domain of Fgfr2 (Fig. 7D). This interdigital channel of low-BrdU cells appeared to be completely absent in PC-*NMyc*$^{f/f}$ limbs (Fig. 8A). Instead, the interdigital tissue of PC-*NMyc*$^{f/f}$ limbs exhibited a more uniform distribution of BrdU-positive cells. A count of BrdU-positive cells within the central core region of interdigital tissue (Fig. 8A) showed 8% of PC and 47% of PC-*NMyc*$^{f/f}$ cells to be positive. We interpret this altered pattern of proliferation to suggest that the central core of low-BrdU and high-Fgfr2 interdigital cells is absent or strongly reduced, resulting in juxtaposition of high-BrdU perichondrial regions of PC-*NMyc*$^{f/f}$ digits in the interdigital space. Along with the altered arrangement of BrdU-positive cells, TEM revealed an altered interdigital architecture in PC-*NMyc*$^{f/f}$ paws, where the loosely packed and apoptotic cells seen in control IDM was replaced by a more homogeneous population of cells with a morphology similar to that of perichondrial cells (Fig. 8C).

As an additional readout for the spacing between digit primordia, we examined blood vessels in the autopod, which form along tracts running adjacent to the digit primordia (Ambler et al., 2001) and delineate the interdigital space. In striking contrast to control limbs, there was very little or no space between blood vessel tracts of adjacent digits in PC-*NMyc*$^{f/f}$ limbs, as marked by Pecam staining (Fig. 8C). These data are consistent with the idea that the diminished or altered expression of BMPs, *Msx2*, *Fgfr2* and *Twist* in the mutant autopod is not caused by their transcriptional downregulation in the absence of N-Myc, but is related to the absence of a channel of interdigital tissue in which they are normally expressed.

DISCUSSION

Our results demonstrate that N-Myc is required for multiple aspects of limb development. These include an early function in regulating the size of precartilaginous condensations in the limb bud and a later requirement for digit individualization and joint formation. The failure of digit separation and joint morphogenesis is associated with a complete absence of programmed cell death in IDM and presumptive joints. From our data, we propose a model, depicted in Fig. 9, in which the small size of precartilaginous condensations caused by *N-Myc* deficiency is linked to the subsequent absence of interdigital cell death. Consistent with reduced proliferation of early limb bud mesenchyme and reduced Sox9 expression observed in *N-Myc*-deficient limb buds, we hypothesize that N-Myc regulates the pool size of FGF-dependent undifferentiated mesenchymal cells (Sun et al., 2002; Boulet et al., 2004). The reduced cell number and corresponding reduction in cell density provide an explanation for the small Sox9-positive precartilaginous condensation and the small skeletal elements that subsequently form in the absence of N-Myc. How would this be linked to the syndactyly that subsequently develops? We propose that the IDM cells targeted for elimination during digit separation are derived from the pool of undifferentiated mesenchyme that exists in the early limb bud. Consistent with this notion, it is well documented that IDM cells, like the undifferentiated mesenchyme of the limb bud, possess chondrogenic potential (Hurle and Ganan, 1986; Ros et al., 1997). We therefore speculate that the decreased number of undifferentiated mesenchymal cells in the early limb bud of PC-*NMyc*$^{f/f}$ mice leads to their depletion as limb development proceeds and is responsible for the absence of a central channel of interdigital tissue, normally marked by the expression of *Fgfr2* and *Msx2* (Fig. 7D,E). The absence or severe reduction in undifferentiated IDM cells normally targeted for cell death as part of the program leading to digit separation provides an explanation for the profound syndactyly that develops. Inherent in this model is the idea that elimination of

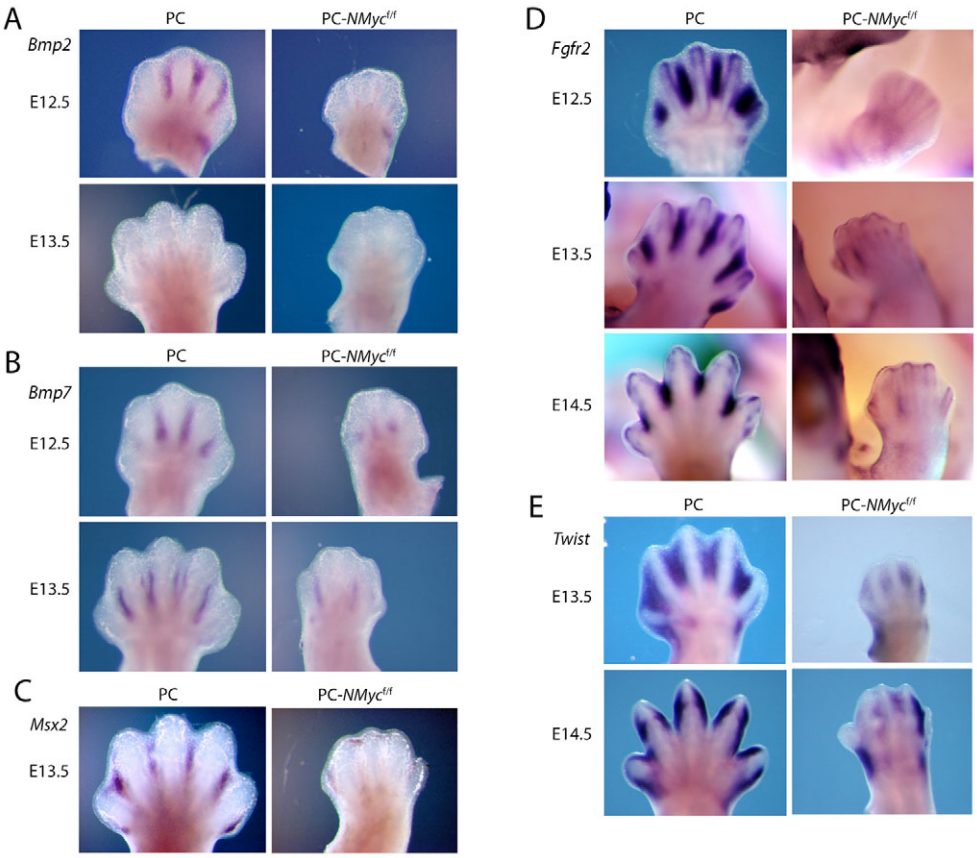

Fig. 7. Diminished or altered expression of interdigital and perichondrial markers in N-Myc-deficient mouse forelimbs. (**A-E**) Whole-mount in situ hybridization analysis for expression of the indicated genes was performed at the indicated embryonic stages.

interdigital mesenchyme normally serves both to initiate digit separation and to remove undifferentiated mesenchymal cells that might otherwise form ectopic cartilage or other structures after the skeletal template is established. Definitive proof of this model will require fate mapping of early limb bud mesenchyme (e.g. Vargesson et al., 1997), performed in conjunction with markers specific for undifferentiated mesenchyme, interdigital tissue and cartilage.

The absence or deficiency in interdigital tissue caused by loss of N-Myc may also underlie the brachydactyly and defective joint formation observed. Cell-tracing studies have demonstrated that interdigital cells, presumably with chondrogenic potential, contribute to forming digits (Omi et al., 2000). Moreover, interdigital BMP expression can influence digit identity (Drossopoulou et al., 2000; Dahn and Fallon, 2000), and the altered BMP, *Msx2* and *Twist* expression in the interdigital tissue of PC-*NMyc*$^{f/f}$ autopods may contribute to the defects in growth and segmentation of digit primordia. Further, interdigital BMP expression appears to be under the control of Shh (Drossopoulou et al., 2000), raising the possibility that N-Myc functions downstream of Shh signaling in either controlling the expression of molecules that determine AP patterning, or in generating/maintaining the cells that express these factors. However, the transient expression of *Gremlin* and *Fgf4*, which function downstream of Shh in the limb bud, are robust in the absence of N-Myc. Indeed, the expansion of *Gremlin* expression may be an underlying mechanism responsible for the small precartilaginous condensations, as Gremlin is a potent inhibitor of BMP-mediated chondrogenesis (Merino et al., 1999). Thus, unlike neuronal precursors, where Shh appears to control both *N-Myc* gene expression and N-Myc protein function (Kenney et al., 2003), N-Myc expression and activity in the developing limb appears to be dissociated from at least some important features of Shh signaling.

Implications for models of proximodistal patterning

Exactly how specification of limb cartilage elements takes place in space and time is under debate, but two models are generally used to explain this complicated process. The progressive specification or progress zone model posits that positional value is specified in cells as a function of the length of time spent in the distal mesenchyme or progress zone (Summerbell et al., 1973). Cells that spend the least time in the progress zone (and perhaps divide a fewer number of times) give rise to more proximal structures, and as the limb grows, more distal structures are produced from cells that have spent more time in the progress zone. More recently, analyses of limb development following AER removal in the chick (Dudley et al., 2002) and following deletion of *Fgf4* and *Fgf8* in the mouse limb (Sun et al., 2002; Boulet et al., 2004) have suggested an alternative model in which cells that give rise to the different proximodistal parts of the limb are specified in the early limb bud and expand during limb outgrowth (reviewed by Mariani and Martin, 2003; Niswander, 2003; Tickle, 2003). Our data indicate that reduced proliferation of undifferentiated limb bud mesenchyme caused by N-Myc deficiency leads to a decrease in the size of the initial condensation in the limb bud and leads to a relatively uniform decrease in the size of all limb skeletal elements (depicted in Fig. 9). If the pool of chondrogenic cells is reduced in these limb buds as predicted, then according to the progress zone model, distal truncations (and normal-sized proximal elements) should occur due to depletion of the progenitor population over time. Although loss of N-Myc causes defects in segmentation of distal elements, their size is not significantly reduced relative to proximal elements. Thus, our data appear not to support the progress zone model and instead are more in line with a pre-specified model for proximodistal

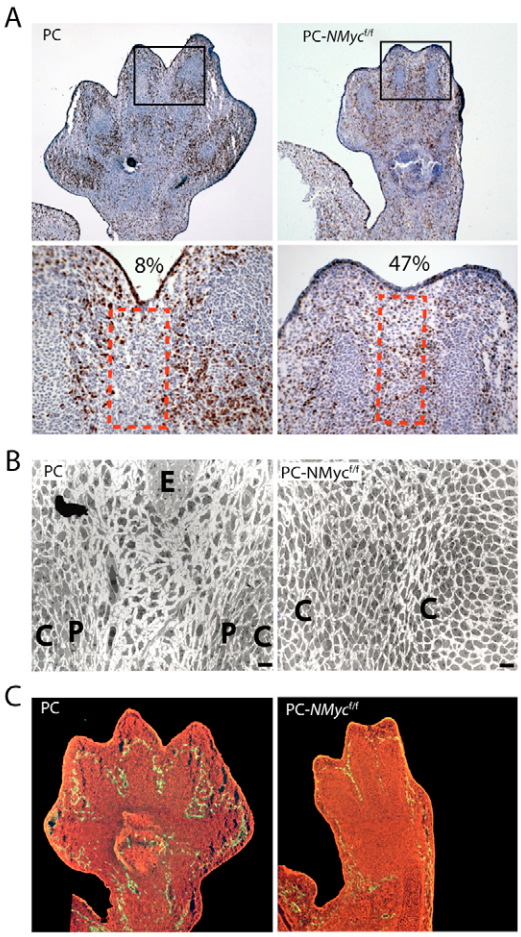

Fig. 8. Loss of interdigital tissue in N-Myc-deficient mouse limbs. (**A**) Staining for BrdU incorporation at E13.5. Note the interdigital channel of predominantly BrdU-negative cells of PC limbs is lost in interdigital regions of PC-*NMyc*$^{f/f}$ limbs. The boxed regions are shown at higher magnification and the percentage of BrdU-positive cells in the specific regions marked by red boxes is indicated. (**B**) TEM of interdigital regions in PC and PC-*NMyc*$^{f/f}$ paws. Scale bars: 10 μm. (**C**) Staining for the blood vessel marker Pecam (green) with propidium iodide. C, cartilage condensations; P, perichondrium; E, epithelium.

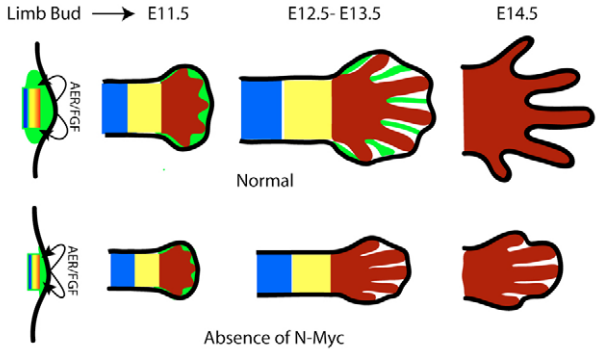

Fig. 9. Model linking skeletal size determination with digit separation in the developing mouse limb. In this model [adapted from Mariani and Martin (Mariani and Martin, 2003)], N-Myc acts downstream of AER-derived FGFs in regulating the pool of undifferentiated mesenchyme (green) in the early limb bud. The undifferentiated mesenchyme gives rise to precartilaginous condensations that are pre-specified to generate proximal [stylopod: forelimb humerous (blue)], medial [zeugopod: forelimb radius and ulna (yellow)] and distal (autopod, red) skeletal elements. After contributing to the growth of the limb segments, residual undifferentiated cells are localized to the IDM, where they contribute to the final stages of autopod patterning and are then eliminated by programmed cell death. Their elimination terminates autopod patterning and initiates digit separation. In the absence of N-Myc, the pool of undifferentiated mesenchymal cells is reduced, leading to a proportional decrease in all skeletal segments. The reduced pool of undifferentiated mesenchymal cells is depleted during skeletal outgrowth, leading to loss of the undifferentiated IDM that is targeted for cell death and required for digit separation.

patterning. However, the relatively severe defects in patterning of the digits caused by N-Myc deficiency suggest that the mechanism responsible for patterning the autopod (or digits) may be connected to, but distinct from, the process that patterns more proximal elements (e.g. radius/ulnar and humerus). Indeed, the notion that patterning of the autopod is performed, at least in part, as a separate episode during limb development has been previously suggested (Tickle, 2003).

Role of N-Myc in human syndactyly syndromes

Despite the identification of many of the disease genes responsible for causing syndactyly, there is very little known about the underlying mechanisms involved. Syndactyly is associated with many different, but often related, human disease syndromes and there is a wide range of severity. Syndactyly in Feingold syndrome, caused by *N-Myc* haploinsufficiency, is typically mild (Celli et al., 2003). Indeed, we do not observe syndactyly following *Prx1*-Cre mediated deletion of a single copy of *N-Myc*. Two of the most common syndactyly-associated syndromes are Apert syndrome and Saethre-Chotzen syndrome. Whereas Apert syndrome is caused by gain-of-function mutations in *Fgfr2* (reviewed by Wilkie et al., 2002), Saethre-Chotzen syndrome is typically caused by haploinsufficiency of *Twist*, but is also sometimes caused by *Fgfr2* and *Fgfr3* mutations (Paznekas et al., 1998). The syndactyly associated with Apert syndrome is often severe (Temtamy and McKusick, 1978) and sometimes approaches the profound syndactyly caused by *Prx1*-Cre mediated deletion of both copies of *N-Myc* described here. Furthermore, there are other defects found in the hands and feet of Apert syndrome patients that are remarkably similar to those caused by loss of *N-Myc*. For example, both feature a very close proximity of the digits, especially the central digits, and a corresponding decrease in the space (tissue) between digits. Both also feature metacarpal fusions at the base of digits 4 and 5, and the absence of distal phalangeal joints and associated brachydactyly (Fig. 3B,C) (Wilkie et al., 2002). Interestingly, *Prx1*-Cre is active in cranial mesenchyme (Logan et al., 2002) and PC-*NMyc*$^{f/f}$ mice exhibit cranial defects (Fig. 1A and not shown) that closely resemble those associated with Apert, Saethre-Chotzen and related syndromes (S.O., Z.Q.Z. and P.J.H., unpublished). Taken together, these phenotypic similarities suggest that N-Myc, Fgfr2 and Twist function in the same pathway(s) responsible for syndactyly and craniosynostosis in Apert and Saethre-Chotzen syndromes (and perhaps other syndromes as well). Moreover, while syndactyly is widely discussed in the context of defects in cell death pathways, our results instead suggest that the underlying mechanism leading to syndactyly in these and perhaps other syndromes may be related to a deficiency of N-Myc-dependent interdigital cells that are targeted for cell death and required for digit separation.

We thank C. Tabin for helpful comments on the manuscript, R. Eisenman and M. Logan for mice, C. Tabin, R. Schweitzer, S. Stadler and R. Eisenman for plasmids and S. Tufa for assistance with TEM. This work was supported by grants to P.J.H. from Shriners Hospitals for Children and the NIH.

References

Ambler, C. A., Nowicki, J. L., Burke, A. C. and Bautch, V. L. (2001). Assembly of trunk and limb blood vessels involves extensive migration and vasculogenesis of somite-derived angioblasts. *Dev. Biol.* **234**, 352-364.

Archer, C. W., Dowthwaite, G. P. and Francis-West, P. (2003). Development of synovial joints. *Birth Defects Res. C Embryo Today* **69**, 144-155.

Bi, W., Deng, J. M., Zhang, Z., Behringer, R. R. and de Crombrugghe, B. (1999). Sox9 is required for cartilage formation. *Nat. Genet.* **22**, 85-89.

Boulet, A. M., Moon, A. M., Arenkiel, B. R. and Capecchi, M. R. (2004). The roles of Fgf4 and Fgf8 in limb bud initiation and outgrowth. *Dev. Biol.* **273**, 361-372.

Brent, A. E., Schweitzer, R. and Tabin, C. J. (2003). A somitic compartment of tendon progenitors. *Cell* **113**, 235-248.

Capdevila, J., Tsukui, T., Esteban, V., Zappavigna, J. and Belmont, C. I. (1999). Control of vertebrate limb outgrowth by the proximal factor Meis2 and distal antagonism of BMPs by Gremlin. *Mol. Cell* **4**, 839-849.

Celli, J., van Bokhoven, H. and Brunner, H. G. (2003). Feingold syndrome: clinical review and genetic mapping. *Am. J. Med. Genet.* **122**, 294-300.

Dahn, R. D. and Fallon, J. F. (2000). Interdigital regulation of digit identity and homeotic transformation by modulated BMP signaling. *Science* **289**, 438-441.

Drossopoulou, G., Lewis, K. E., Sanz-Ezquerro, J. J., Nikbakht, N., McMahon, A. P., Hofmann, C. and Tickle, C. (2000). A model for anteroposterior patterning of the vertebrate limb based on sequential long- and short-range Shh signalling and Bmp signalling. *Development* **127**, 1337-1348.

Dudley, A. T., Ros, M. A. and Tabin, C. J. (2002). A re-examination of proximodistal patterning during vertebrate limb development. *Nature* **418**, 539-544.

Fallon, J. F., Lopez, A., Ros, M. A., Savage, M. P., Olwin, B. B. and Simandl, B. K. (1994). FGF-2: apical ectodermal ridge growth signal for chick limb development. *Science* **264**, 104-107.

Guha, U., Gomes, W. A., Kobayashi, T., Pestell, R. G. and Kessler, J. A. (2002). In vivo evidence that BMP signaling is necessary for apoptosis in the mouse limb. *Dev. Biol.* **249**, 108-120.

Hurle, J. M. and Ganan, Y. (1986). Interdigital tissue chondrogenesis induced by surgical removal of the ectoderm in the embryonic chick leg bud. *J. Embryol. Exp. Morphol.* **94**, 231-244.

Hurlin, P. J. (2005). N-myc functions in transcription and development. *Birth Defects Res. C Embryo Today* **75**, 340-352.

Kato, K., Kanamori, A., Wakamatsu, Y., Sawai, S. and Kondoh, H. (1991). Tissue distribution of N-myc expression in the early organogenesis period of the mouse embryo. *Dev. Growth Differ.* **33**, 29-36.

Kenney, A. M., Cole, M. D. and Rowitch, D. H. (2003). Nmyc upregulation by sonic hedgehog signaling promotes proliferation in developing cerebellar granule neuron precursors. *Development* **130**, 15-28.

Knoepfler, P. S., Cheng, P. F. and Eisenman, R. N. (2002). N-myc is essential during neurogenesis for the rapid expansion of progenitor cell populations and the inhibition of neuronal differentiation. *Genes Dev.* **16**, 2699-2712.

Logan, M., Martin, J. F., Nagy, A., Lobe, C., Olson, E. N. and Tabin, C. J. (2002). Expression of Cre Recombinase in the developing mouse limb bud driven by a Prxl enhancer. *Genesis* **33**, 77-80.

Lu, P., Minowada, G. and Martin, G. R. (2006). Increasing Fgf4 expression in the mouse limb bud causes polysyndactyly and rescues the skeletal defects that result from loss of Fgf8 function. *Development* **133**, 33-42.

Mariani, F. V. and Martin, G. R. (2003). Deciphering skeletal patterning: clues from the limb. *Nature* **423**, 319-325.

Merino, R., Rodriguez-Leon, J., Macias, D., Ganan, Y., Economides, A. N. and Hurle, J. M. (1999). The BMP antagonist Gremlin regulates outgrowth, chondrogenesis and programmed cell death in the developing limb. *Development* **126**, 5515-5522.

Murphy, M. J., Wilson, A. and Trumpp, A. (2005). More than just proliferation: Myc function in stem cells. *Trends Cell Biol.* **15**, 128-137.

Nilsson, J. A. and Cleveland, J. L. (2003). Myc pathways provoking cell suicide and cancer. *Oncogene* **22**, 9007-9021.

Niswander, L. (2003). Pattern formation: old models out on a limb. *Nat. Rev. Genet.* **4**, 133-143.

Okubo, T., Knoepfler, P. S., Eisenman, R. N. and Hogan, B. L. (2005). Nmyc plays an essential role during lung development as a dosage-sensitive regulator of progenitor cell proliferation and differentiation. *Development* **132**, 1363-1374.

Omi, M., Sato-Maeda, M. and Ide, H. (2000). Role of chondrogenic tissue in programmed cell death and BMP expression in chick limb buds. *Int. J. Dev. Biol.* **44**, 381-388.

Paznekas, W. A., Cunningham, M. L., Howard, T. D., Korf, B. R., Lipsonm, M. H., Grix, A. W., Feingold, M., Goldberg, R., Borochowitz, Z., Aleck, K. et al. (1998). Genetic heterogeneity of Saethre-Chotzen syndrome, due to TWIST and FGFR mutations. *Am. J. Hum. Genet.* **62**, 1370-1380.

Queva, C., Hurlin, P. J., Foley, K. P. and Eisenman, R. N. (1998). Sequential expression of the MAD family of transcriptional repressors during differentiation and development. *Oncogene* **16**, 967-977.

Ros, M. A., Piedra, M. E., Fallon, J. F. and Hurle, J. M. (1997). Morphogenetic potential of the chick leg interdigital mesoderm when diverted from the cell death program. *Dev. Dyn.* **208**, 406-419.

Sakai, L. Y., Keene, D. R., Morris, N. P. and Burgeson, R. E. (1986). Type VII collagen is a major structural component of anchoring fibrils. *J. Cell Biol.* **103**, 1577-1586.

Sawai, S., Kato, K., Wakamatsu, Y. and Kondoh, H. (1990). Organization and expression of the chicken N-myc gene. *Mol. Cell. Biol.* **10**, 2017-2026.

Sawai, S., Shimono, A., Wakamatsu, Y., Palmes, C., Hanaoka, K. and Kondoh, H. (1993). Defects of embryonic organogenesis resulting from targeted disruption of the N-myc gene in the mouse. *Development* **117**, 1445-1455.

Soriano, P. (1999). Generalized lacZ expression with the ROSA26 Cre reporter strain. *Nat. Genet.* **21**, 70-71.

Summerbell, D., Lewis, J. H. and Wolpert, L. (1973). Positional information in chick limb morphogenesis. *Nature* **244**, 492-496.

Sun, X., Mariani, F. V. and Martin, G. R. (2002). Functions of FGF signalling from the apical ectodermal ridge in limb development. *Nature* **418**, 501-508.

te Welscher, P., Fernandez-Teran, M., Ros, M. A. and Zeller, R. (2002). Mutual genetic antagonism involving GLI3 and dHAND prepatterns the vertebrate limb bud mesenchyme prior to SHH signaling. *Genes Dev.* **16**, 421-426.

Temtamy, S. A. and McKusick, V. A. (1978). The genetics of hand malformations. *Birth Defects Orig. Artic. Ser.* **14**, i-xviii, 1-619.

Tickle, C. (2003). Patterning systems – from one end of the limb to the other. *Dev. Cell.* **4**, 449-458.

van Bokhoven, H., Celli, J., van Reeuwijk, J., Rinne, T., Glaudemans, B., van Beusekom, E., Rieu, P., Newbury-Ecob, R. A., Chiang, C. and Brunner, H. G. (2005). MYCN haploinsufficiency is associated with reduced brain size and intestinal atresias in Feingold syndrome. *Nat. Genet.* **37**, 465-467.

Vargesson, N., Clarke, J. D., Vincent, K., Coles, C., Wolpert, L. and Tickle, C. (1997). Cell fate in the chick limb bud and relationship to gene expression. *Development* **124**, 1909-1918.

Wang, C. K., Omi, M., Ferrari, D., Cheng, H. C., Lizarraga, G., Chin, H. J., Upholt, W. B., Dealy, C. N. and Kosher, R. A. (2004). Function of BMPs in the apical ectoderm of the developing mouse limb. *Dev. Biol.* **269**, 109-122.

Wilkie, A. O., Patey, S. J., Kan, S. H., van den Ouweland, A. M. and Hamel, B. C. (2002). FGFs, their receptors, and human limb malformations: clinical and molecular correlations. *Am. J. Med. Genet.* **112**, 266-278.

Zucker, R. M., Hunter, E. S., 3rd and Rogers, J. M. (1999). Apoptosis and morphology in mouse embryos by confocal laser scanning microscopy. *Methods* **18**, 473-480.

Zuniga, A., Haramis, A.-P. G., McMahon, A. P. and Zeller, R. (1999). Signal relay by BMP antagonism controls the SHH/FGF4 feedback loop in vertebrate limb buds. *Nature* **401**, 598-602.

Zuzarte-Luis, V. and Hurle, J. M. (2005). Programmed cell death in the embryonic vertebrate limb. *Semin. Cell Dev. Biol.* **16**, 261-269.